Supplementary Material

Thermodynamic and structural relationships between the two polymorphs of 1,3-dimethylurea

Christian Näther, Cindy Döring, Inke Jess, Peter G. Jones and Christina Taouss

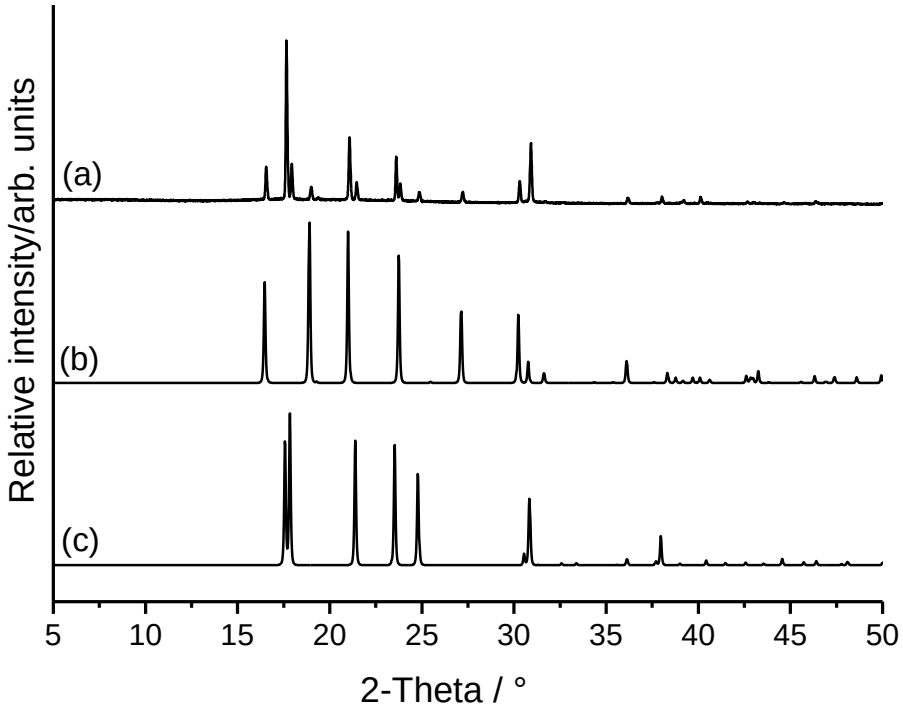

Fig. S1. X-ray powder pattern of the batch that contains the fibrous needles (a) and of form II (b) and form I (c) calculated from single crystal data measured at room-temperature.

Fig. S2. Microscopic image of the batch containing the fibrous needles.

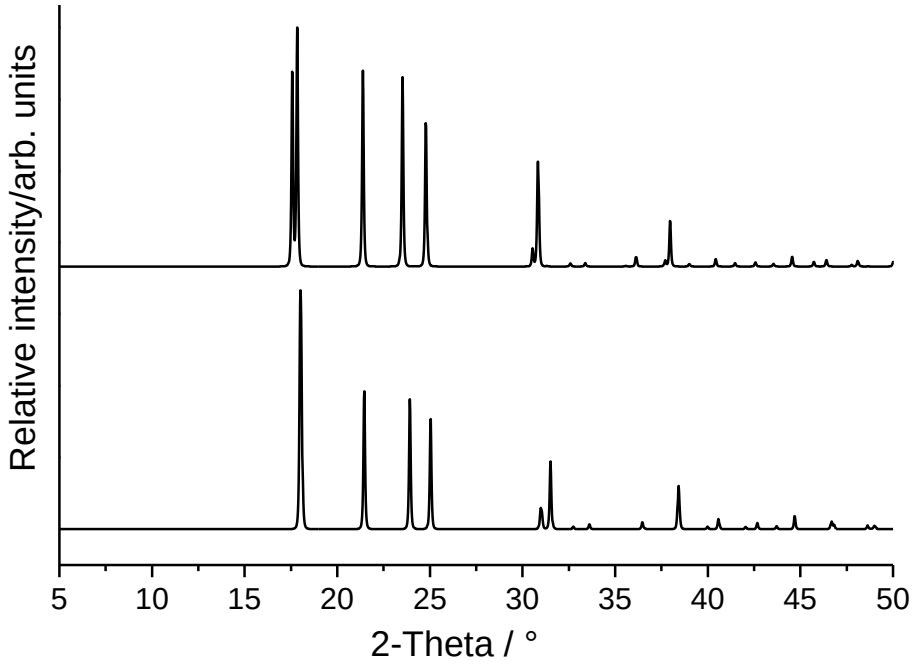

Fig. S3. X-ray powder pattern of polymorph I calculated from single crystal data measured at room-temperature (top) and at 180K (bottom)

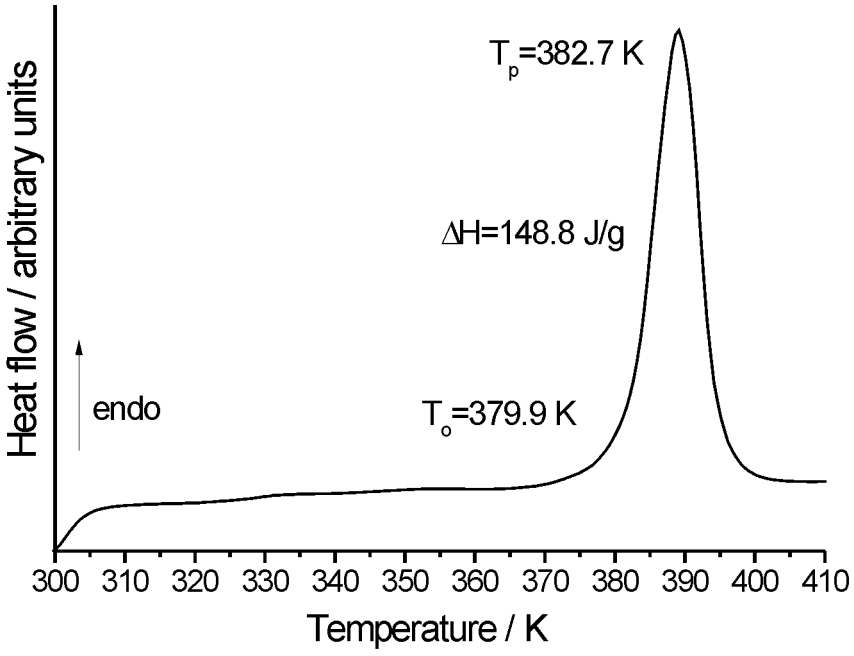

Fig. S4: X-ray powder pattern of polymorph II calculated from single crystal data measured at room-temperature (top) and at 100K (bottom).

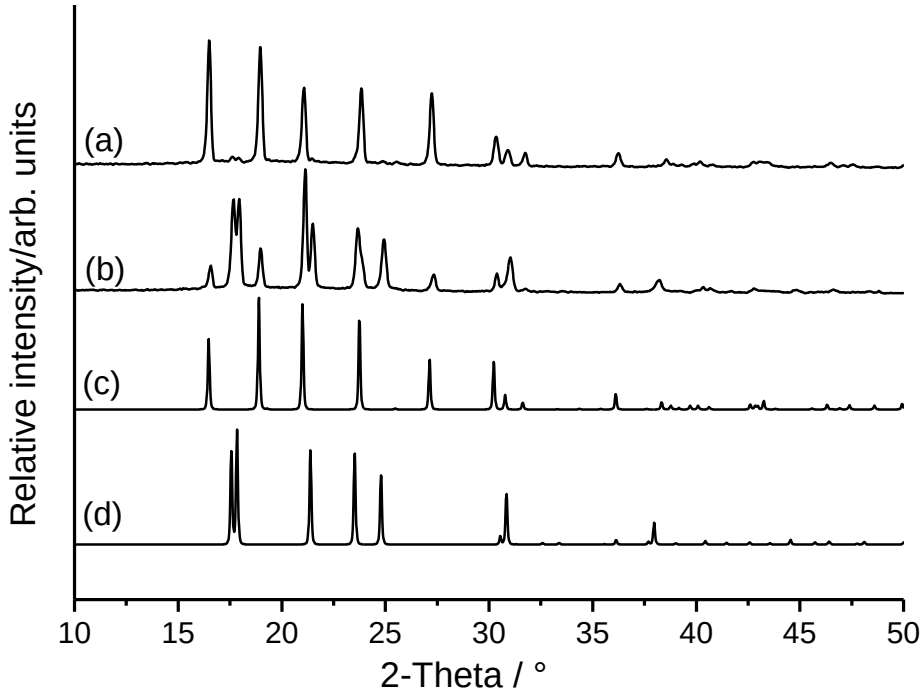

Fig. S5: X-ray powder pattern of the commercially available compound (a), of the residue isolated at 50°C (b) and calculated pattern of polymorph II (c) and polymorph I (d).

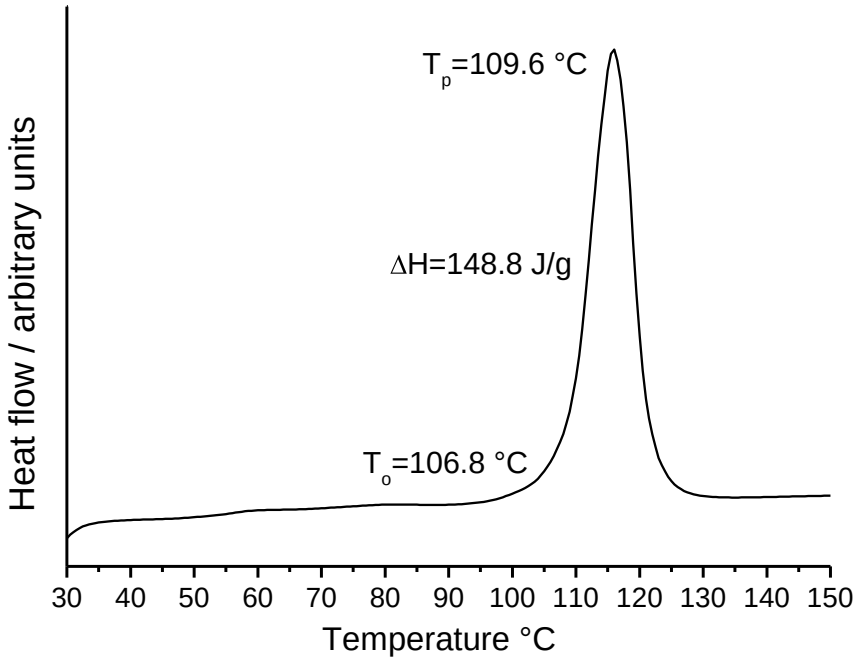

Fig. S6: DSC curve of polymorph II (T_o = extrapolated onset temperature; T_p = peak temperature; heating rate 30°C/min).

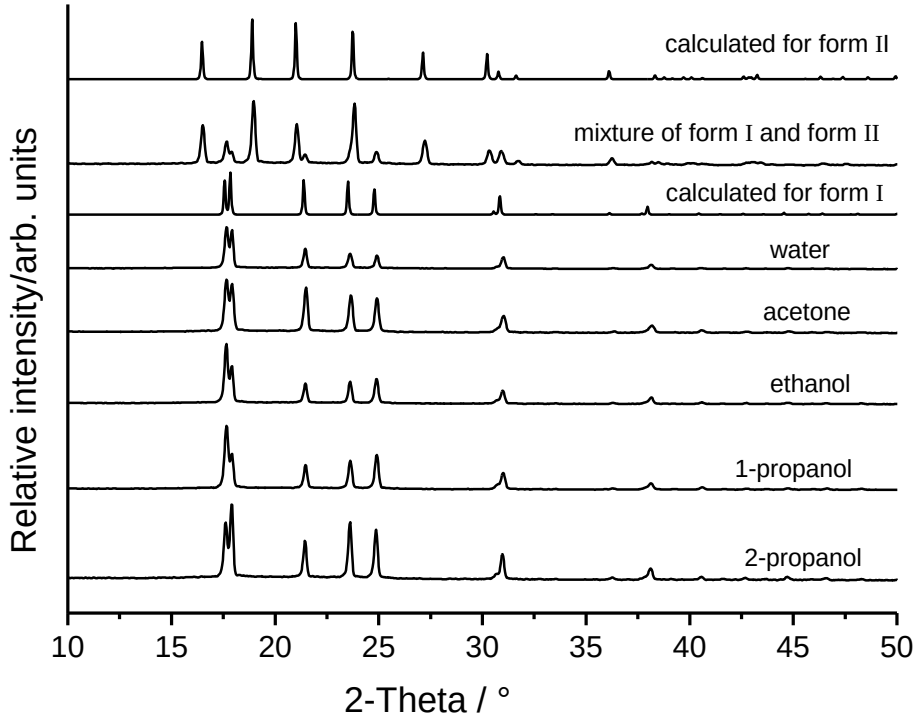

Fig. S7: X-ray powder patterns of the residues formed in the solvent-mediated conversion experiments using water, acetone, ethanol, 1-propanol and 2-propanol, together with that of the pristine material and that calculated for polymorph I and polymorph II.

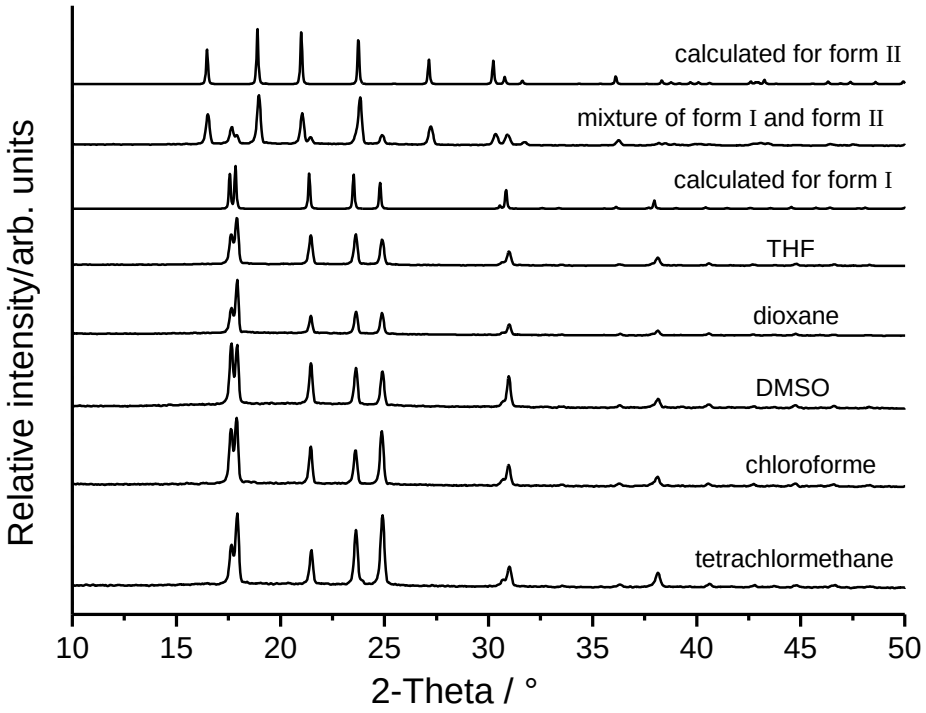

Fig. S8: X-ray powder patterns of the residues formed in the solvent-mediated conversion experiments using THF, dioxane, DMSO, chloroform and tetrachloromethane together with that of the pristine material and that calculated for polymorph I and polymorph II.

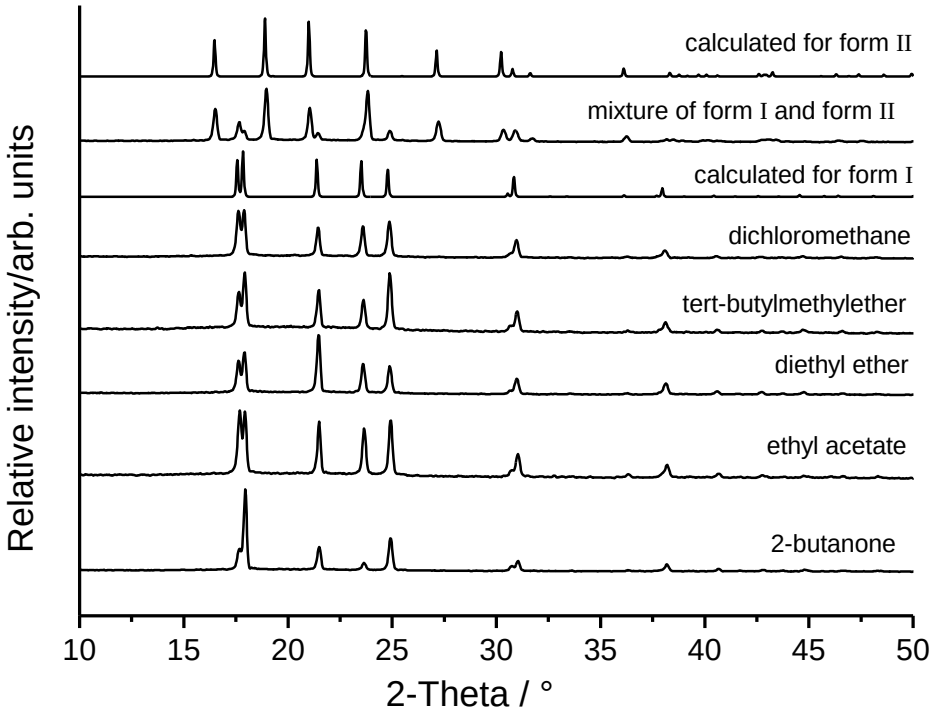

Fig. S9: X-ray powder patterns of the residues formed in the solvent mediated conversion experiments using dichloromethane, tert.-butyl methyl ether, diethyl ether, ethyl acetate and 2-butanone, together with that of the pristine material and that calculated for polymorph I and polymorph II.

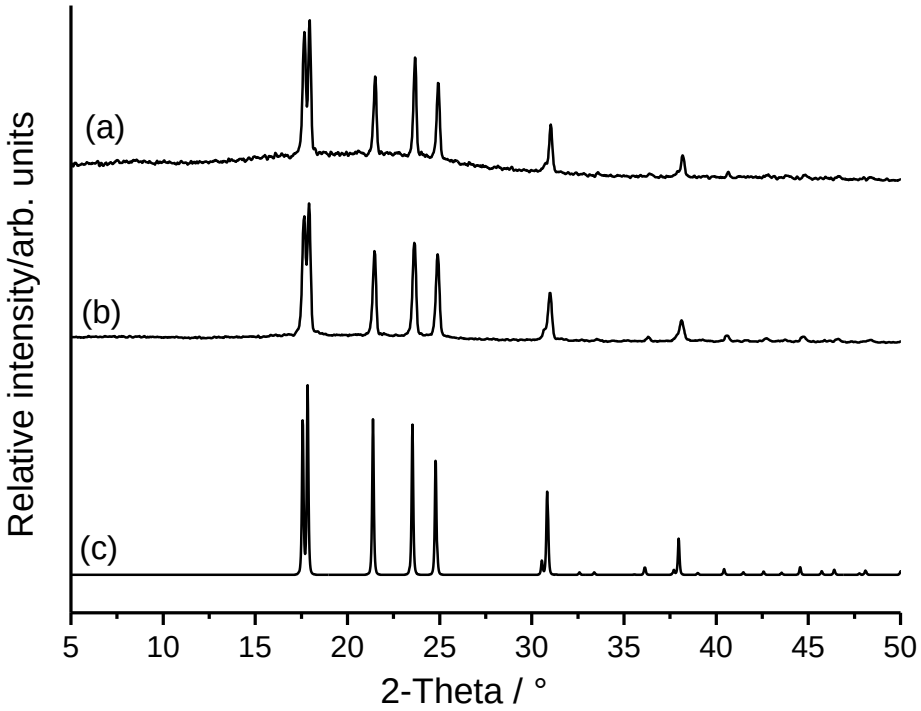

Fig. S10: Experimental powder patterns of the residue obtained by fast removal of the solvent of a saturated solution in diethyl ether (a), of the residue obtained by cooling the melt in liquid nitrogen (b) and calculated powder pattern for polymorph I (c).

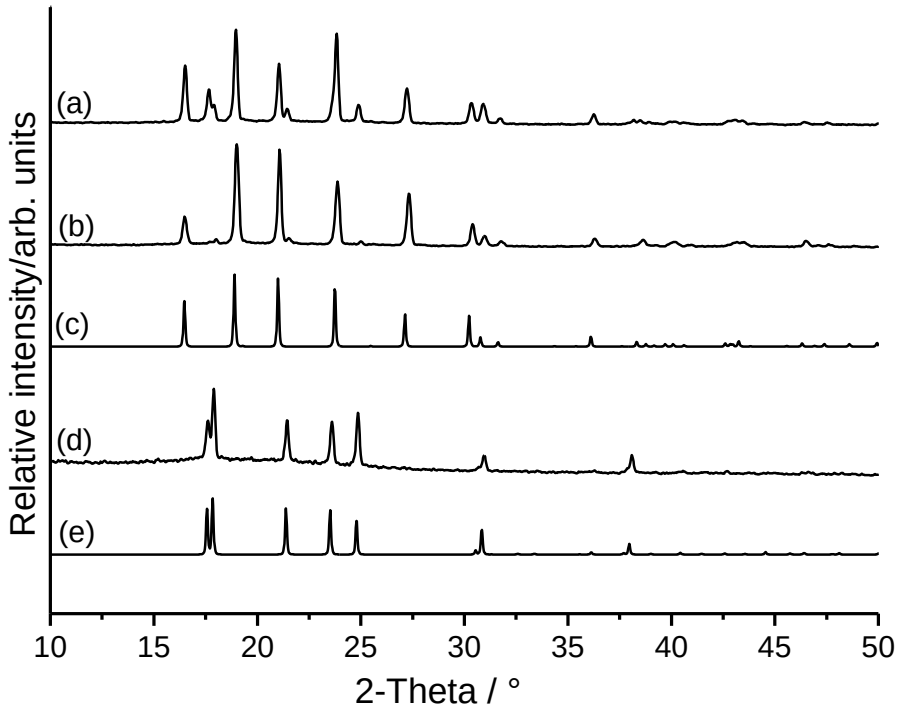

Fig. S11: Experimental X-ray powder patterns of a mixture of polymorph I and polymorph II (a), of the residue obtained after storing this mixture in a refrigerator at 4°C for 3 d in acetone (b) of the residue obtained after storing this mixture for 3 d at room temperature in acetone (d), with calculated powder patterns for polymorph II (c) and polymorph I (e).

Table S1. Crystal data and structure refinement for I and II at room temperature.

Polymorph	I	II
Empirical formula	$C_3H_8N_2O$	$C_3H_8N_2O$
Formula weight	88.11	88.11
Temperature (K)	293	293
Wavelength (Å)	0.71073	0.71073
Crystal system	Orthorhombic	Orthorhombic
Space group	*Fdd*2	$P2_12_12$
Unit cell dimensions (Å): *a*	11.4161(18)	10.7542(13)
b	20.178(4)	5.2159(9)
c	4.5709(9)	4.5968(5)
Volume ($Å^3$)	1052.9(3)	257.85(6)
Z	8	2
Density (calculated) (Mg/m^3)	1.112	1.135
μ (mm^{-1})	0.08	0.09
F(000)	384	96
$2\theta_{max}$	56.3	56.4
Reflections collected	2176	3835
Independent reflections	354 [*R*(int) = 0.048]	388 [*R*(int) = 0.092]
Data / restraints / parameters	354 / 1 / 34	388 / 0 / 34
Goodness-of-fit on F^2	1.17	1.27
Final *R* indices [*I*>2sigma(*I*)]	*R*1 = 0.055, *wR*2 = 0.106	*R*1 = 0.047, *wR*2 = 0.134
R indices (all data)	*R*1 = 0.104, *wR*2 = 0.122	*R*1 = 0.050, *wR*2 = 0.137
Largest diff. peak / hole (e $Å^{-3}$)	0.06 / –0.07	0.09 / –0.10